AGU PUBLICATIONS

Geophysical Research Letters

Supporting Information for

How important are diapycnal mixing and geothermal heating for the deep circulation of the Western Mediterranean?

Bruno Ferron[1], Pascale Bouruet Aubertot[2], Yannis Cuypers[2], Katrin Schroeder[3], Mireno Borghini[4]

[1]Univ. Brest, CNRS, IFREMER, IRD, Laboratoire d'Océanographie Physique et Spatiale, IUEM, Brest, France

[2]LOCEAN-UPMC, LOCEAN, Paris, France

[3]CNR ISMAR – Arsenale, Tesa 104, Castello 2737/F, 30122 Venice, Italy

[4]CNR-ISMAR, Sede di La Spezia, Forte Santa Teresa, 19036 Pozzuolo di Lerici, Italy

Contents of this file

Introduction

The supporting information contains some supplementary details about the method used to relate the diapycnal velocity to the dissipation rate and the eddy diffusivity. It presents studies that estimated deep water formation rates in the western Mediterranean Sea. It also contains two figures and two tables. Figure S1 shows vertical profiles of turbulent kinetic energy dissipation rates by region as defined on Fig. 1a. Figure S2 presents the ~~probablity~~probability density function of the bathymetric roughness for the whole western Mediterranean basin and at the microstructure stations. Table S1 presents studies that estimated the annual mean deep water formation rate in the western Mediterranean Sea. Table S2 presents the seven oceanographic cruises that contributed to the microstructure dataset used in this study. Table S3 presents the amplitude of the right hand side terms of Eqn. S1.

1. Method

The diapycnal velocity w_d^K associated with the vertical turbulent diffusion K due to small-scale turbulence was diagnosed using the potential density "conservation" equation [*McDougall*, 1991]:

$$w_d^K \frac{1}{\rho_\theta}\partial_z\rho_\theta = \partial_z\left(K\frac{1}{\rho_\theta}\partial_z\rho_\theta\right) + K\left[\left(\partial_z\theta\right)^2\partial_\theta\alpha + \partial_z\theta\,\partial_z S\left(\partial_S\alpha - \partial_\theta\beta\right) - \left(\partial_z S\right)^2\partial_S\beta\right], \quad \text{(S1)}$$

T1 T2 T3 T4 T5

where ∂_x denotes a partial derivative with respect to the variable x, z is the vertical direction, ρ_θ is the potential density referenced to an appropriate pressure p_r, θ is the potential temperature and S the salinity, α (β) is the thermal expansion (haline contraction) coefficient referenced to the same pressure p_r. The first term on the right-hand side (T1) is the vertical divergence of the turbulent density flux. Among the extra terms between square brackets, *McDougall and You* [1990] showed that the first term (T2) may be of the same order of magnitude as (T1) depending on the region that is considered. For the western ~~Med~~Mediterranean, all terms between brackets are at least two orders of magnitude smaller than (T1) below 800 m (Table S3). Note that compared to *McDougall’s* [1991]~~'s~~ Eqn. 20, variations of α with S and of β with S and θ were considered. Furthermore, since we are interested in diagnosing how turbulence can induce a loss of buoyancy at depth, we only considered the terms associated with the vertical diffusion and disregarded the potential increase of buoyancy due to cabelling effects caused by lateral diffusion.

Using direct numerical simulations, *Shih et al.* [2005] and *Bouffard and Boegman* [2013] identified four regimes of turbulent vertical diffusivity that depend on the turbulent intensity parameter $Re_b=\varepsilon/(\nu N^2)$, where N is the buoyancy frequency and ν is the kinematic viscosity: the molecular regime ($Re_b < 1.7$) for which the turbulent diffusivity K is equal to the molecular diffusivity, the buoyancy-controlled regime ($1.7 < Re_b < 8.5$) for which $K=0.1\ Pr^{-1/4}\nu Re_b^{1/2}$ and Pr is the Prandtl number, the transition regime ($8.5 < Re_b < 400$) for which $K=\Gamma\varepsilon N^{-2}$ with a constant mixing efficiency Γ of 0.2 [*Osborn*, 1980], and the energetic regime ($Re_b > 400$) for which $K=4\nu Re_b^{1/2}$. The boundaries between the various regimes are given for $Pr = 7$ and are supported by field data [*Bouffard and*

Boegman, 2013]. Applying the widely used Osborn relationship in the energetic regime would overestimate the eddy diffusivity [*Shih et al.*, 2005]. In this study, Re_b was first derived from the dissipation rate and the buoyancy frequency measured by the VMP, which determined the relevant relationship for the diffusivity. Among the distinct stations that were occupied, the transition regime accounts for 60% of the dissipation rate estimates while the energetic regime accounts for 32%.

Combining (1) and the expressions for diffusivity leads to:

$$w_d^K = \Gamma N^{-2} \partial_z \epsilon \text{ , in the transition regime} \quad \text{(S2)}$$

$$w_d^K = 4 N^{-2} \partial_z \left(\nu^{1/2} \epsilon^{1/2} N \right) \text{ , in the energetic regime} \quad \text{(S3)}$$

Thus, in the transition regime and in the energetic regime with a quasi-uniform stratified fluid, the sign of the diapycnal velocity only depends on the sign of the vertical gradient of the turbulent kinetic energy dissipation rate. In the energetic regime with a depth-varying stratification, the vertical gradient in buoyancy frequency needs to be accounted for to determine the sign of the diapycnal velocity.

2. Estimates of the western Mediterranean deep water (DW) formation rate

Several estimates of the annual mean DW formation rate are found in the literature (Table S1). A large range of values is found since, if DW formation rates clearly depend on the severity of winter conditions and on the preconditioning of the stratification, they also depend on the methods, density/depth thresholds used to estimate the volume of newly formed dense waters.

Using monthly climatological air-sea fluxes and sea surface temperature and salinity, *Tziperman and Speer* [1994] estimated the amount of water modified by the surface buoyancy fluxes. They found that 1–1.5 Sv of surface waters were transformed into waters having DW characteristics. Since the method does not provide the proportion of those dense waters that sink at depth, this formation rate is an upper bound of the actual DW formation rate. Using the same approach, *Lascaratos* [1993] estimated an annual DW formation rate of 0.3 Sv. *Rhein* ~~*et al.*~~ [1995] used a box model that simulated chlorofluoromethane and tritium distributions to estimate that an annual mean 2.6–3.6 Sv of WMDW was injected below 1000 m from 1945 to 1992. Building on indirect observations of the stratification from an acoustic tomography array complemented by conductivity-temperature-depth (CTD) profiles, *Send et al.* [1995] estimated that 0.3 Sv of WMDW was injected below 1000 m during the 1991–1992 winter. *Schroeder et al.* [2008] used the large scale temperature-salinity distribution from CTD casts covering the western ~~Med~~Mediterranean to estimate the volume of the specific new WMDW formed from 2004 to 2006. They found a yearly formation rate of 2.4 Sv for $\sigma_0 > 29.107$ kg m^{-3} for those two years, including open-sea convection and dense shelf water cascading. *Durrieu de Madron et al.* [2013] estimated an open-sea formation rate of 1.1 Sv ($\sigma_0 >$ 29.126 kg m^{-3}) for winter 2011–2012 from observations of vertical profiles of temperature and salinity and the horizontal distribution of chlorophyll-a concentration. From current-meter arrays located in several canyons, they estimated that dense shelf water cascading injected 0.07 Sv at depth, an estimate comparable to the 2004–2005 estimate by *Ulses et al.* [2008] from a primitive equation model with a 1.5 km horizontal resolution. A dense shelf water cascading reaching 0.03 Sv was estimated from current-meter observations and temperature-salinity distribution in the western basins for winter 1998–1999 [*Bethoux et al.*, 2002]. Using CTD casts and a reconstruction method from an observing system simulation experiment, *Waldman et al.* [2016] estimated that 1.8–2.8 Sv of water denser than 29.11 kg m^{-3} were formed during the 2012–2013 winter, a value in the same range as the 2004-2006 estimate by *Schroeder et al.* [2008] for $\sigma_0 > 29.107$ kg m^{-3}. From winter 2008–2009 to 2012–2013, *Houpert et al.* [2016] found from the MOOSE observation network that deep convection reached the bottom each year and that water denser than 29.11 kg m^{-3} was formed at a minimum annual rate of 1.14, 0.91 and 1.25 Sv for winters 2008–2009, 2009–2010 and 2011–2012 respectively. These latter annual rates are lower bound estimates due to the use of the chlorophyll-a images (see [*Houpert et al.*, 2016] for further details). No deep convection was found during winter 2007–2008. Using a coupled ocean-atmosphere model for the 1980–2013 period, *Somot et al.* [2016] found that 5 years formed DWs ($\sigma_0 > 29.10$ kg m^{-3}) at a rate larger than 0.6 Sv, 14 years at a rate within 0.05 – 0.6 Sv and 14 years at a rate within 0–0.05 Sv. The average 1980–2013 DW formation rate was 0.3 Sv. For recent years, which had the largest number of observations, the model sometimes underestimated the DW formation rates estimated from observations: 0.9 Sv for winters 2004–2006 (vs 2.4 Sv from observations), 1.1 Sv (vs 1.1) for 2008-2009, 0.3 Sv (vs 0.9) for 2009–2010, 0.9 Sv (vs 1.2) for 2011–2012, 1.7 Sv (vs 1.8–2.8) for 2012–2013. A lack of horizontal model resolution, errors in the atmospheric forcings, hydrostatic representation of nonhydrostatic convective processes, but also errors in formation rates estimated from observations are all a source of discrepancy. Nonetheless, the model study provides interesting information on the time variability of the DW formation. Consistently with the model, assuming that the four winters 2000–2002 and 2006–2008 did not formed any DWs ($\sigma_0 > 29.11$ kg m^{-3}), that winter 2002–2003 formed as much DW as winter 2009–2010, that winter 2003-2004 formed one fourth of the 2002-2003 rate, and using DW formation rates estimated from observations, a mean formation rate of 0.93 Sv is found for 13 winters of the 2000-2013 period. The standard deviation representing the interannual variability is as large (0.9 Sv). According to those estimates, we assume in this study that the most probable long-term average yearly DW formation rates ranges from 0.3 to 0.9 Sv.

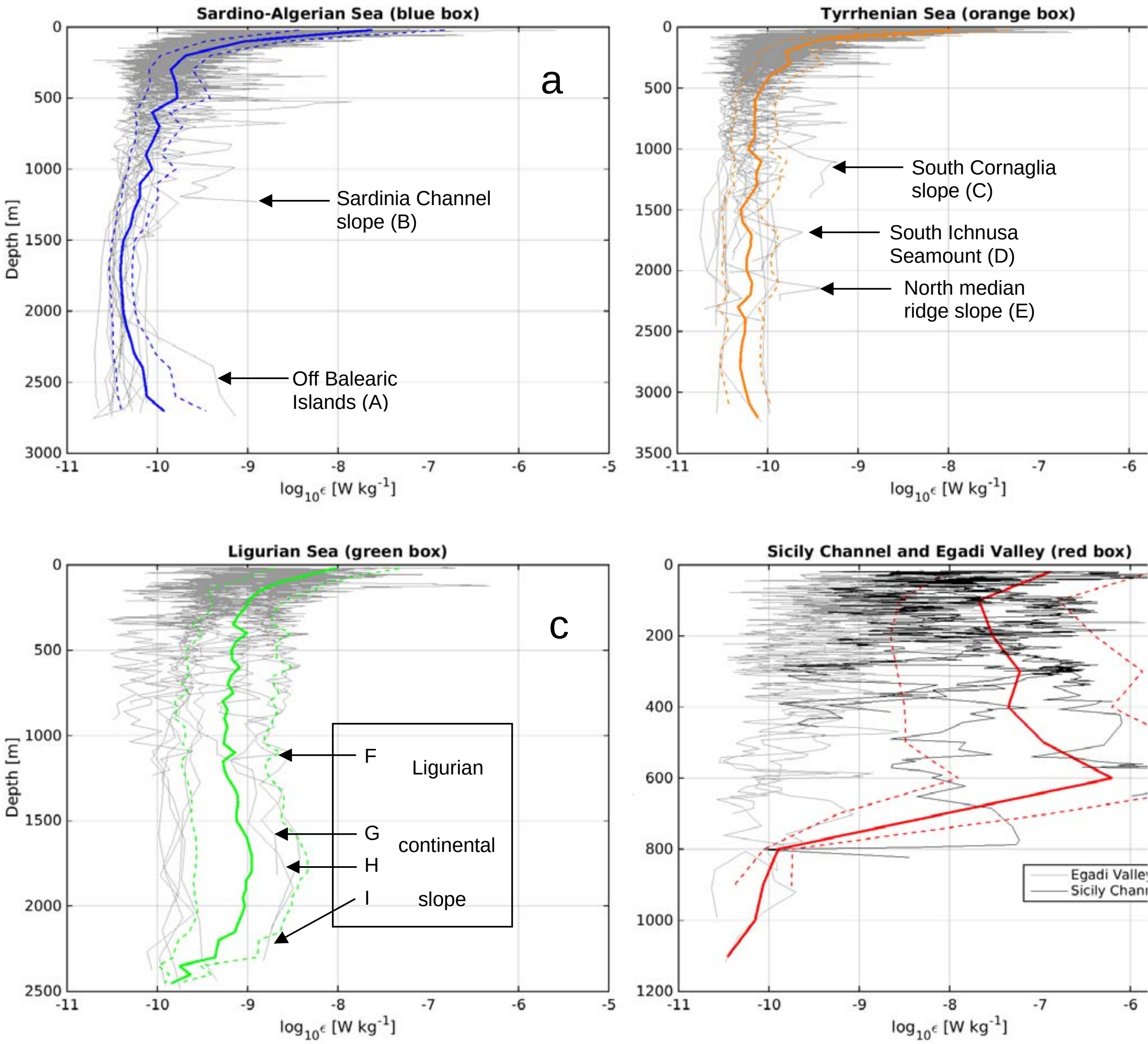

Figure S1. Vertical profiles of turbulent kinetic energy dissipation rates (thin light and dark gray) and their average (thick coloured) as a function of the regional boxes defined on Fig. 1a (same region-color coding). The scatter of the profiles (dashed coloured) around their mean was calculated as the rms of the ratio between the profiles and their average. Arrows denote some specific turbulence intensified profiles that are located on Fig. 1b.

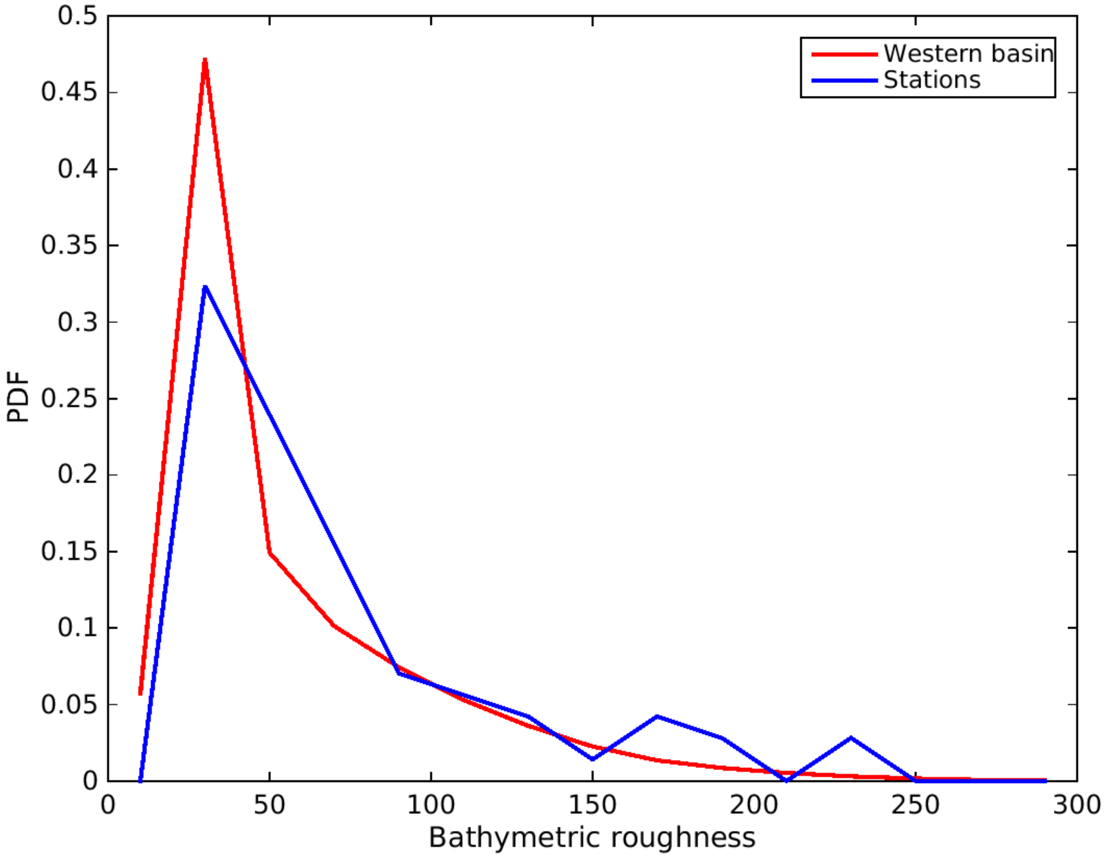

Figure S2. Probability density function (PDF) of the bathymetric roughness for the whole western Mediterranean basin and the local microstructure stations.

Study	Period	Annual mean rate of dense water formation (Sv)	Location and properties
Lascaratos (1993)	Mean estimate from climatology	0.3	Open sea – Gulf of Lion ($\sigma_0 >$ 28.92 kg m^{-3})
Tziperman and Speer (1994)	Mean estimate from climatology	1 – 1.5	Open sea – Western Med. ($\sigma_0 >$ 29.0 kg m^{-3})
Send et al. (1995)	Winter 1991–1992 from tomography	0.3	Open Sea, Gulf of Lion, below 1000 m
Rhein (1995)	1945 –1992 mean from CFM concentrations	2.6 – 3.6	Open sea, upper bound for waters exported below 1000 m
Bethoux (2002)	Winter 1998–1999 from θ –S distribution	0.03	Cascading from the shelf
Schroeder et al. (2008)	Winters 2004-2006 from θ –S distribution	2.4	Open sea, below 1800 m, $\sigma_1 >$ 33.477 kg m^{-3} ($\sigma_0 >$ 29.107 kg m^{-3})
Durrieu de Madron (2013)	Winter 2011-2012 open ocean : from θ –S and chlorophyll-a distribution. shelf cascading: from current-meters.	1.1 0.07	Open sea, $\sigma_0 >$ 29.126 kg m^{-3} Cascading from the Gulf of Lion and Catalan shelves
Waldman et al. (2016)	Winter 2012-2013 open ocean from CTD casts and an observing system simulation experiment using MOOSE network	1.1 – 1.7 1.8 – 2.8	Open sea, $\sigma_0 >$ 29.11 kg m^{-3} , restricted to MOOSE network domain Extrapolated to the whole northwestern basin
Houpert et al. (2016)	Observations from MOOSE network and sea surface chlorophyll-a distribution. Winter 2008-2009 Winter 2009-2010 Winter 2011-2012	 1.14 0.91 1.25	Open-sea $29.114 < \sigma_0 < 29.116$ kg m^{-3} $29.116 < \sigma_0 < 29.119$ kg m^{-3} $29.119 < \sigma_0 < 29.126$ kg m^{-3}
Ulses et al. (2008)	Winter 2004-2005 Ocean modeling study	0.07	Cascading from Gulf of Lion and Catalan shelves
Somot et al. (2016)	Winters 1980 to 2013 Coupled ocean-atmosphere modeling study atmosphere: 50-km resolution ocean: 10-km resolution	> 0.6: 5 years 0.05 – 0.6: 14 years 0 – 0.05: 14 years	Open sea, $\sigma_0 >$ 29.10 kg m^{-3}

Table S1. Annual mean deep water formation rate (Sv, 1 Sv = 10^6 m^3 s^{-1}) in the western Mediterranean Sea from various studies.

Cruise name	Date	Research Vessel	Number of full-depth VMP profiles
DRUMB	20/04/2012-26/04/2012	Europe	6
VAD	27/11/2013-03/12/2013	Europe	8
VENUS	04/06/2013-25/06/2013	Urania	25
ICHNUSSA 2013	14/10/2013-30/10/2013	Urania	26
MEDOCC	24/03/2014-10/04/2014	Urania	30
EMSO	26/06/2014-04/07/2014	Urania	13
ICHNUSSA 2014	13/11/2014-01/12/2014	Urania	40

Table S2. Oceanographic cruises that contributed to the microstructure data set used in this study.

Region	Depth Range [m]	T2/T1	T3/T1	T4/T1	T5/T1
Ligurian Sea	100-800	3×10^{-1}	2×10^{-2}	2×10^{-2}	4×10^{-4}
	800-1300	3×10^{-2}	2×10^{-3}	2×10^{-3}	4×10^{-5}
	> 1300	9×10^{-3}	4×10^{-4}	4×10^{-4}	8×10^{-6}
Sardino-Algerian Sea	200-600	2×10^{-2}	7×10^{-4}	6×10^{-4}	2×10^{-5}
	600-1300	5×10^{-2}	2×10^{-3}	2×10^{-3}	4×10^{-5}
	> 1300	3×10^{-4}	4×10^{-5}	3×10^{-5}	3×10^{-6}
Tyrrhenian Sea	100-500	1×10^{-2}	5×10^{-4}	5×10^{-4}	2×10^{-4}
	500-1300	4×10^{-2}	2×10^{-3}	2×10^{-3}	4×10^{-5}
	>1300	2×10^{-2}	1×10^{-3}	1×10^{-3}	2×10^{-5}

Table S3. Example of the root mean squared value of the terms between brackets scaled by the first term on the right and side of Eqn. S1 for three depth ranges of the regions whose depth is larger than 1000 m. Changes in the order of magnitude of the T1 term were used to determined depth ranges.